# Eigenmode Distortion as a Novel Criterion for Motion Cueing Fidelity in Rotorcraft Flight Simulation

MiletoviC, Ivan; Pavel, Marilena; Stroosma, Olaf; Pool, Daan; van Paassen, Rene; Wentink, Mark; Mulder, Max

**Publication date**
2018

**Document Version**
Final published version

**Published in**
Proceedings of the 44th European Rotorcraft Forum

**Citation (APA)**
MiletoviC, I., Pavel, M., Stroosma, O., Pool, D., van Paassen, R., Wentink, M., & Mulder, M. (2018). Eigenmode Distortion as a Novel Criterion for Motion Cueing Fidelity in Rotorcraft Flight Simulation. In C. Hermans (Ed.), *Proceedings of the 44th European Rotorcraft Forum: Delft, The Netherlands, 2018* Article 45

European Rotorcraft Forum

# EIGENMODE DISTORTION AS A NOVEL CRITERION FOR MOTION CUEING FIDELITY IN ROTORCRAFT FLIGHT SIMULATION

Ivan Miletović[1], Marilena D. Pavel[1], Olaf Stroosma[1], Daan M. Pool[1], Marinus M. van Paassen[1], Mark Wentink[2], and Max Mulder[1]

[1]Delft University of Technology, Kluyverweg 1, 2629HS Delft, The Netherlands
{I.Miletovic,M.D.Pavel,O.Stroosma,D.M.Pool,M.M.vanPaassen,M.Mulder}@tudelft.nl
[2]Desdemona B. V., Kampweg 5, 3769DE Soesterberg, The Netherlands
mark.wentink@desdemona.eu

**Abstract**

Eigenmode distortion (EMD) is a novel methodology developed to study the degradation of perceived vehicle dynamics as a result of motion cueing algorithms (MCA's) applied in rotorcraft flight simulators. This paper briefly introduces EMD and subsequently describes its application in a pilot-in-the-loop experiment conducted on the SIMONA Research Simulator at Delft University of Technology. The experiment considers a precision hover task performed by two test pilots in three different motion cueing conditions. Each of the evaluated conditions is devised such to best reproduce one of the vehicle modes (pitch/heave subsidences and phugoid) simulated using an independently developed, three degree-of-freedom, longitudinal, non-linear model of the AH-64 Apache helicopter. The experiment yielded a number of interesting results. For example, the mode participation factors (MPFs) computed using recorded model states showed that the unstable phugoid mode dominates the overall dynamic response in all conditions evaluated. Also, based on the relative distribution of MPF's across the three motion conditions, some indication of a change in pilot control behaviour as a result of motion cues (or lack thereof) was exposed. Finally, subjective pilot ratings suggest that the motion cueing condition optimized for the pitch subsidence mode is preferred, even though this is not the dominant mode in the vehicle's response. The condition corresponding to the heave subsidence mode (i.e., only vertical motion cues) is appreciated least.

## 1 INTRODUCTION

Over the years, there have been many efforts to develop objective means for motion system tuning and fidelity assessment in flight simulation[1,15,18,19]. One of the most recent and probably promising tools is the Objective Motion Cueing Test (OMCT)[8,9], now included as part of the ICAO standards for fixed-wing aircraft full-flight simulators[3]. The OMCT measures the (linear) dynamics of the motion cueing system (MCS), which is responsible for constraining a moving-base simulator to its available workspace by means of the motion cueing algorithm (MCA). In the OMCT, the MCA is driven by a prescribed set of test signals aimed at evaluating *frequency responses* of the MCS. Combined, these frequency responses characterize the linear dynamic behaviour of the complete MCS over a frequency range of interest.


Figure 1: The SIMONA Research Simulator at Delft University of Technology.

Although state-of-the-art criteria[3] based on OMCT are still in the process of being validated[21], recently a number of optimization algorithms based on OMCT or equivalent frequency-domain metrics were proposed[6,10]. While some promising results, supported by subjective pilot ratings, were recently reported[11], such approaches face two main challenges. First, the cost functions and weighing factors inherent in optimization schemes often lack in transparency and are subject to significant engineering judgment. An often reported difficulty is establishing appropriate trade-offs in the relative importance of motion in the different simulator axes and for different tasks[10,16]. Moreover, the existing methods consider the motion cueing system in isolation and do not take into account the dynamic interaction with the *vehicle dynamics model*. In particular, the coupling of motion in different vehicle degrees-of-freedom is often overlooked. Motion cueing signals have interactions that are determined by the vehicle dynamics model and task, which also affect the often non-linear and coupled MCA dynamics. Recent work has indeed demonstrated that tailoring the currently prescribed OMCT test signals[3,8] to account for vehicle- and task-specific properties yields significant variations in the obtained frequency responses[5]. As part of an ongoing research project jointly organised by Delft University of Technology and Desdemona B.V. (operator of the Desdemona simulator), a novel technique was developed to expose this intricate three-way interaction between 1) task, 2) vehicle dynamics and 3) motion cueing[12]. This technique, called *eigenmode distortion* (EMD), is able to quantify the MCA induced degradation of human-perceived motion cues with respect to baseline vehicle dynamics, while also more accurately accounting for the dynamic coupling of vehicle degrees-of-freedom.

This paper will discuss the novel approach to MCA tuning in more detail by considering the example of a simple longitudinal three degree-of-freedom generic helicopter flight mechanics model, used to approximate the dynamics of the AH-64 Apache helicopter. Furthermore, to explore the implications of the various assumptions (e.g., linearization) inherent in the proposed methodology, preliminary data from a validation experiment performed by two test pilots in the SIMONA Research Simulator (SRS) at the Delft University of Technology (see Figure 1) is presented.

The paper is structured as follows. First, in Section 2, the EMD methodology is introduced. Then, in Section 3, the validation experiment is discussed after which the obtained results are presented in Section 4. Finally, a discussion is included in Section 5 and the paper is concluded in Section 6.

## 2 METHODOLOGY

The method proposed in this paper relies on the novel concept of *eigenmode distortion* (EMD). Within EMD, the vehicle's dynamic response is decomposed along *decoupled* coordinates known as the vehicle's *eigenmodes*. Helicopter dynamics are often analysed in terms of these modes[14], as they contain crucial information about the vehicle's stability and dynamic response properties.

EMD inherently assumes that the eigenmodes are perceived by the human operator as *characteristic* responses of the system. The dynamics of the Motion Cueing Algorithm (MCA) *distort* these eigenmodes through a combination of scaling and filtering. In order to quantify this distortion, the vehicle and MCA dynamics are *explicitly coupled* in *linear* form using a novel mathematical framework[12]:

$$
\begin{aligned}
\begin{pmatrix} \delta\dot{\bar{x}}^p \\ \delta\dot{\bar{x}}^m \end{pmatrix} &= \begin{bmatrix} A^p & 0 \\ A^{mp} & A^m \end{bmatrix} \begin{pmatrix} \delta\bar{x}^p \\ \delta\bar{x}^m \end{pmatrix} + \begin{bmatrix} B^p \\ 0 \end{bmatrix} \begin{pmatrix} \delta\bar{u}^p \\ 0 \end{pmatrix} \\
&= A^c \delta\bar{x}^c + B^c \delta\bar{u}^c, \\
\begin{pmatrix} \delta\bar{y}^p \\ \delta\bar{y}^m \end{pmatrix} &= \bar{y}^c = C^c \bar{x}^c,
\end{aligned}
\tag{1}
$$

where the vectors $\delta\bar{x}^p$ and $\delta\bar{x}^m$ contain states that describe the evolution of the linearized *vehicle* and *MCA* dynamics, respectively. The matrices $A^p$ and $A^m$ are the respective system matrices corresponding to $\delta\bar{x}^p$ and $\delta\bar{x}^m$. The matrix $A^{mp}$ *couples* the dynamics of both systems, while the coupled system itself is excited solely by the input vector $\delta u^p$ (i.e., the pilot controls) through the matrix $B^p$. The matrices $A^{mp}$ and $A^m$ change as a function of parameters in the MCA, while $A^p$ and $B^p$ change with changing vehicle dynamics (e.g., as a function of forward flight speed). Finally, the coupled system output $\bar{y}^c$ contains both vehicle reference and simulated *human perceived* quantities (i.e., specific forces and angular rates[20]) that are a linear combination, determined by the matrix $C^c$, of the states in $\bar{x}^p$ and $\bar{x}^m$.

### 2.1. Eigenmode distortion criterion

The key innovation of the formulation in Equation (1) is that it accommodates a *modal coordinate transformation*[13]. This transformation enables a systematic analysis of the *distortion* of human perceived quantities induced by the MCA in terms of the vehicle's eigenmodes. Subsequent inspection of the *eigenvectors* within each of these modes can reveal *the extent to which the MCA dynamics affect human perceived specific forces and angular rates per individual mode*[12]. A potential criterion for motion cueing fidelity based on EMD can then be formulated as *pre-*

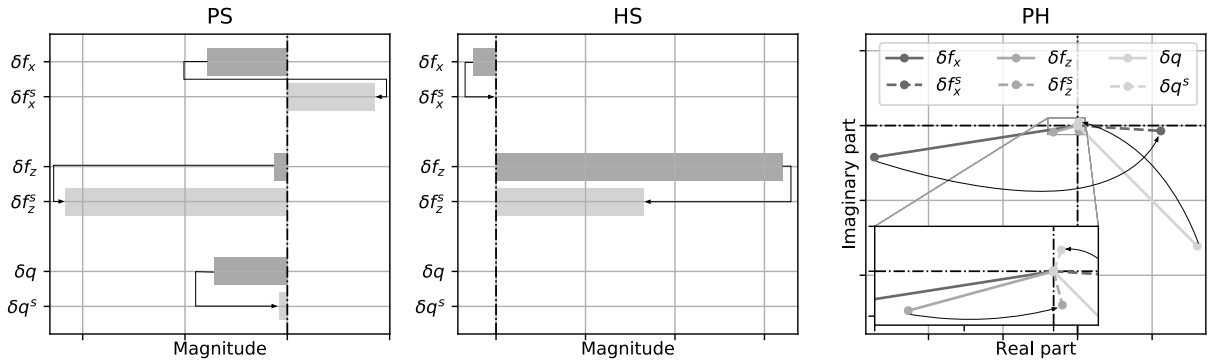


Figure 2: An example of modal distortion induced by the MCA, showing baseline and distorted human-perceived quantities as eigenvectors within each vehicle eigenmode.

*serving the dominant vehicle mode(s) given the available simulator motion space*.

A typical example of modal distortion as a function of MCA parameters is depicted in Figure 2. This figure shows the degradation of baseline vehicle dynamics by the MCA, in terms of human-perceived quantities (i.e., specific forces and rotational rates) within each eigenmode of the vehicle. For a three degree-of-freedom helicopter model, these modes are the pitch subsidence (PS), heave subsidence (HS) and the phugoid (PH). The human-perceived quantities are shown as *normalized eigenvectors* within each respective mode. Hence, the corresponding numerical values along the axes in Figure 2 are omitted as only the *relative* magnitudes of the eigenvectors are of interest.

The pitch and heave subsidences have *real* eigenvalues and therefore the corresponding eigenvectors are also real. This allows for distortion in terms of magnitude and sign only. The distortion of the vehicle's real modes is visualized using horizontal bars in Figure 2. In the figure, baseline vehicle dynamics are represented as specific forces and angular rates perceived by humans, i.e., $\delta f_x$, $\delta f_z$ and $\delta q$, and remain constant with changes in the MCA. The same quantities superscripted with $s$ represent the *distorted* outputs of the linearized MCA. The arrows drawn in the figures corresponding to the pitch and heave subsidences (i.e., PS and HS) indicate the induced magnitude and, possibly, sign changes with respect to the baseline vehicle dynamics.

The phugoid mode has a *complex* eigenvalue and hence, in general, the eigenvectors associated with this mode are also complex. The distortion of a complex mode is characterized by changes in both magnitude and (relative) *phase* of its eigenvectors. A typical distortion of the complex valued phugoid mode is also visualized in Figure 2. The arrows drawn in the complex plane indicate the change in magnitude and phase in each of the individual human-perceived quantities represented by one of the complex eigenvectors. However, it also shows how the *relative* relation between human-perceived quantities in different degrees-of-freedom is affected. For example, it becomes possible to quantify the distortion of the relative magnitude and phase between $\delta f_x$ and $\delta q$ by comparing it to the relative magnitude and phase between $\delta f_x^s$ and $\delta q^s$.

In Section 3, more examples of modal distortion as a function of changes in MCA parameters will be given. There, the motion cueing configurations evaluated in a pilot-in-the-loop experiment conducted on the SRS are discussed in more detail.

### 2.2. Mode participation factors

An open question that needs to be addressed, because it is not possible to minimize the distortion of all vehicle modes at the same time, is how to quantify the *relative importance* of the different modes. This requires knowledge of some fundamental concepts in linear systems theory.

The dynamic response of linear systems can be fully described in terms of *modal coordinates*. In effect, the value of the linear (vehicle) system state, $\delta\bar{x}^p$, excited by external input,s $\delta\bar{u}^p(\tau)$, at any given time, $t$, can be written in terms of the system's eigenvalues and eigenvectors as[14]:

$$\bar{x}^p(t) = \sum_{i=1}^{n} (\bar{v}_i^T \delta\bar{x}_0^p \bar{w}_i)\, e^{\lambda_i^p t} + \sum_{i=1}^{n} \int_0^t \left(\bar{v}_i^T B^p \delta\bar{u}^p(\tau)\bar{w}_i\right) e^{\lambda_i^p (t-\tau)}\, d\tau \tag{2}$$

Equation (2) signifies that the linear system's response can be decomposed into individual contributions corresponding to each of the $n$ system modes. In this equation, $\bar{v}_i^T$ and $\bar{w}_i$ are the *left*

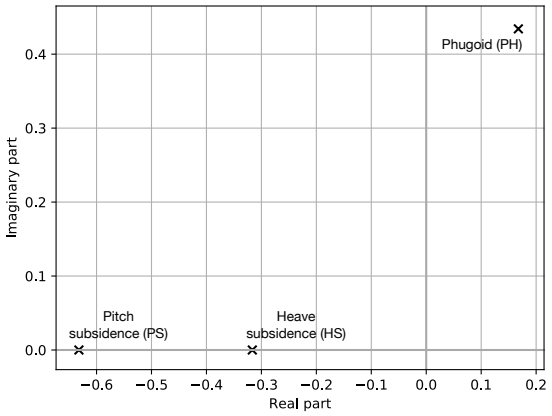


Figure 3: AH-64 model eigenvalues in hover.

Table 1: AH-64 model stability and control derivatives in hover.

| Stability derivatives | | Control derivatives | |
|---|---|---|---|
| $X_u$ | -0.034 | $X_{u_0}$ | 0.025 |
| $X_w$ | 0.023 | $X_{u_s}$ | 0.053 |
| $X_q$ | 0.27 | $Z_{u_0}$ | -0.30 |
| $Z_u$ | 0.022 | $Z_{u_s}$ | 0.0046 |
| $Z_w$ | -0.31 | $M_{u_0}$ | -0.00041 |
| $Z_q$ | 0.024 | $M_{u_s}$ | -0.033 |
| $M_u$ | 0.014 | | |
| $M_w$ | 0.00078 | | |
| $M_q$ | -0.27 | | |

and *right* eigenvectors, respectively, corresponding to the $i$-th eigenvalue of the system, $\lambda_i^p$. Here, the left and right eigenvectors form an *orthonormal* pair that is obtained from:

$$A^p \bar{w}_i = \lambda_i^p \bar{w}_i \qquad \text{and} \qquad \bar{v}_i^T A^p = \bar{v}_i^T \lambda_i^p \tag{3}$$

from which it becomes apparent that $\bar{v}_i^T$ multiplies the system matrix *left* and $\bar{w}_i$ multiplies the system matrix *right*. The eigenvectors form the basis of the *modal coordinate transformation*. In this transformation, a vector $\delta\bar{r}^p(t)$ is defined for each state $\delta\bar{x}^p(t)$ such that:

$$\delta\bar{x}^p(t) = W\,\delta\bar{r}^p(t) = \begin{bmatrix} \bar{w}_1 & \bar{w}_2 & \cdots & \bar{w}_{n-1} & \bar{w}_n \end{bmatrix} \bar{r}^p(t) \tag{4}$$

Hence, a state $\delta\bar{x}^p(t)$ can be obtained in terms of its modal coordinates using:

$$\delta\bar{r}^p(t) = W^{-1}\,\delta\bar{x}^p(t) = \begin{bmatrix} \bar{v}_1^T \\ \bar{v}_2^T \\ \vdots \\ \bar{v}_{n-1}^T \\ \bar{v}_n^T \end{bmatrix} \delta\bar{x}^p(t) \tag{5}$$

The vector $\bar{r}^p(t)$ therefore expresses the response of the system along its individual and *decoupled* modes. The elements of $\bar{r}^p(t)$ are, in general, complex valued. However, a measure of the *magnitude*, or *participation*, of each individual mode to the system's response can be obtained from the absolute value of the elements in $\bar{r}^p(t)$.

Given a sequence of vehicle states $\delta\bar{x}^p$ at arbitrary times $t$ in a manoeuvre, a scalar measure of the extent to which each vehicle mode is excited in a particular manoeuvre can be obtained from:

$$m_i = \int_0^T |r_i(t)|\,dt \qquad \forall \qquad i \in (1, n) \tag{6}$$

where $m_i$ is defined as the *mode participation factor* (MPF) of the $i$-th mode and $T$ is the duration of the executed manoeuvre. Comparison of the magnitudes of individual MPFs thus yields the relative importance of each *mode*. This knowledge can be valuable as an *objective guide* in the design and configuration of MCAs.

## 3 EXPERIMENT SETUP

To investigate the applicability of the EMD criterion, an experiment was conducted. In this experiment, two military test pilots were invited to perform a hover task in the SRS (see Figure 1). During the experiment several different motion cueing conditions obtained using the EMD method were evaluated. In the following sections, first more detailed information is presented on the helicopter dynamics, task, and evaluated MCA configurations. Then, the *a-priori* experiment hypotheses, dependent measures and experiment procedure are discussed.

### 3.1. Helicopter dynamics

The task was performed using an analytical, nonlinear and generic (longitudinal) three degrees-of-freedom helicopter model with quasi-steady disc-tilt dynamics. This generic model is used in combination with an independently developed parameter set derived to approximate the unaugmented dynamics of the AH-64 Apache helicopter. Figure 3 and Table 1 show the dynamic modes in hover as well as the associated stability and control derivatives, respectively, computed from this model.

### 3.2. Task

The task that the pilots were asked to perform is the hover Mission Task Element (MTE) described in ADS-33E[2]. The helicopter degrees-of-freedom are constrained to the longitudinal motion only and, hence, the stipulated task requirements only apply to these three degrees-of-freedom. To simplify the analysis, the transition phase in the original manoeuvre is omitted. Hence, the vehicle starts and should be kept in a stabilized hover for approximately 30 seconds. The following specifications apply[2]:

- Allowed longitudinal position offset: 3 ft (desired) or 6 ft (adequate).
- Allowed altitude offset: 2 ft (desired) or 4 ft (adequate).

In order to ensure sufficient (external) excitation during the task, moderate turbulence is also included. This turbulence is based on the Dryden spectra[4] and perturbs the vehicle only in the longitudinal and vertical directions.

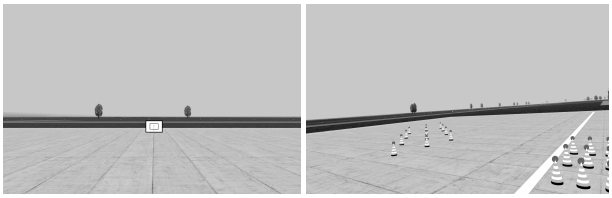

Figure 4: Setup of the hover MTE as seen on the SRS visual system.

Figure 4 shows the setup of the hover task as seen on the SRS visual system. The hover board shown is included primarily as an altitude reference, whereas the pylons on the right are included as longitudinal position references. In this experiment, the absolute measures of task performance are taken as the root mean squares (RMS's) of the longitudinal and vertical position errors.

### 3.3. Motion cueing algorithm

In this paper, the Classical Washout Algorithm (CWA) is used to map the vehicle motion on to the simulator workspace[17]. Figure 5 shows a schematic of the CWA.

In the current experiment, Channel ② (tilt-coordination) is disabled and, since only three (longitudinal) degrees of freedom are active, the roll and sway axes in the CWA are also disabled. In effect, the CWA reduces to a set of three high-pass filters in the pitch, surge and heave axes, respectively. For the present experiment, these filters are selected to be of second order, such that:

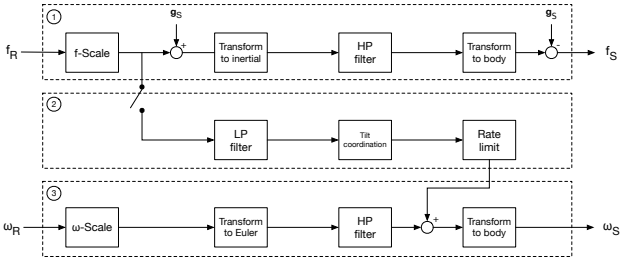


Figure 5: A schematic of the Classical Washout Algorithm[17], with three channels.

$$H_{\square}^{hp} = K_{\square} \frac{s^2}{s^2 + 2\zeta\omega_{n_{\square}} s + \omega_{n_{\square}}^2} \tag{7}$$

Here, the $\square$ is used as a placeholder to denote the respective degrees-of-freedom of the simulator, i.e., $q$ (pitch), $x$ (surge) or $z$ (heave). The damping ratio $\zeta$ is fixed at a value of 1.0 for all simulator degrees of freedom. $K_{\square}$ and $\omega_{n_{\square}}$ are the scaling gains and filter break-frequencies, respectively, and are the only variable parameters in the experiment.

*A-priori*, it is not known which vehicle modes are dominant in the task to be performed, because this depends on the adopted pilot strategy. Hence, it has been opted to devise three motion cueing configurations using EMD, each designed to preserve one of the three vehicle modes, i.e.: the pitch subsidence, heave subsidence and phugoid. These motion conditions are labelled APM (Aperiodic Pitch Motion), AHM (Aperiodic Heave Motion) and PHM (Phugoid Motion), respectively. Table 2 lists the values of the individual parameters in every motion configuration. Figure 6 shows the MCA induced modal distortion corresponding to each configuration. In the following paragraphs, the configurations are discussed in more detail.

Table 2: Motion cueing parameters per experimental condition. Filter break frequencies are in rad/s.

| APM | | AHM | | PHM | |
|---|---|---|---|---|---|
| $K_x$ | 0.3 | $K_x$ | 0.5 | $K_x$ | 0.8 |
| $\omega_{n_x}$ | 1.25 | $\omega_{n_x}$ | 2.0 | $\omega_{n_x}$ | 1.0 |
| $K_z$ | 0.8 | $K_z$ | 1.2 | $K_z$ | 0.2 |
| $\omega_{n_z}$ | 1.2 | $\omega_{n_z}$ | 0.8 | $\omega_{n_z}$ | 2.0 |
| $K_q$ | 1.0 | $K_q$ | 0.5 | $K_q$ | 0.8 |
| $\omega_{n_q}$ | 0.0 | $\omega_{n_q}$ | 2.0 | $\omega_{n_q}$ | 0.5 |

**No motion (NM)** A reference condition without simulator motion was included in the experiment to assess task performance improvement in comparison to the three conditions with simulator motion.

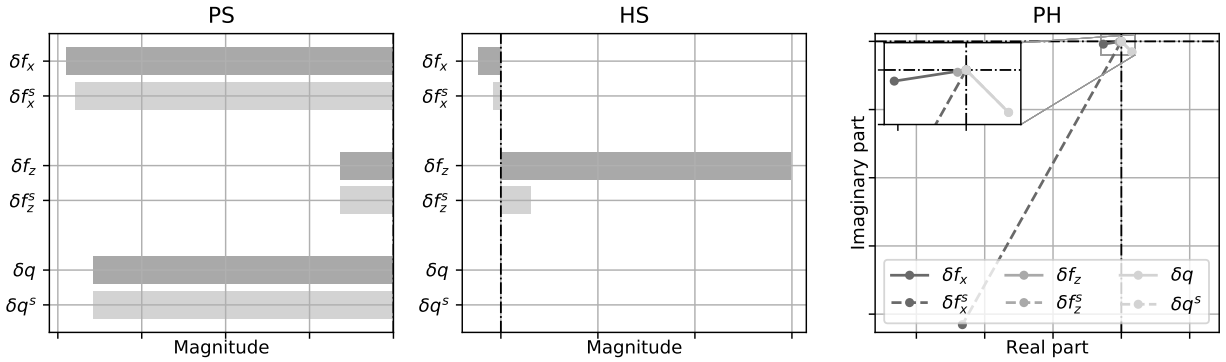


(a) APM

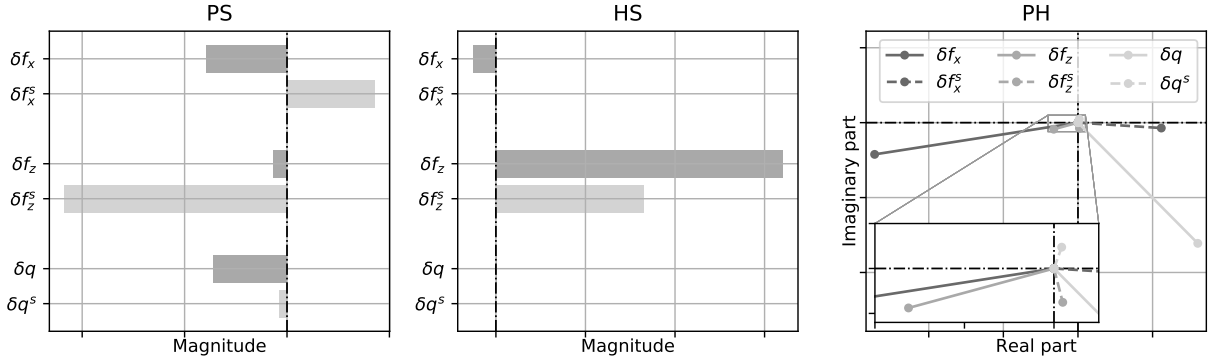


(b) AHM

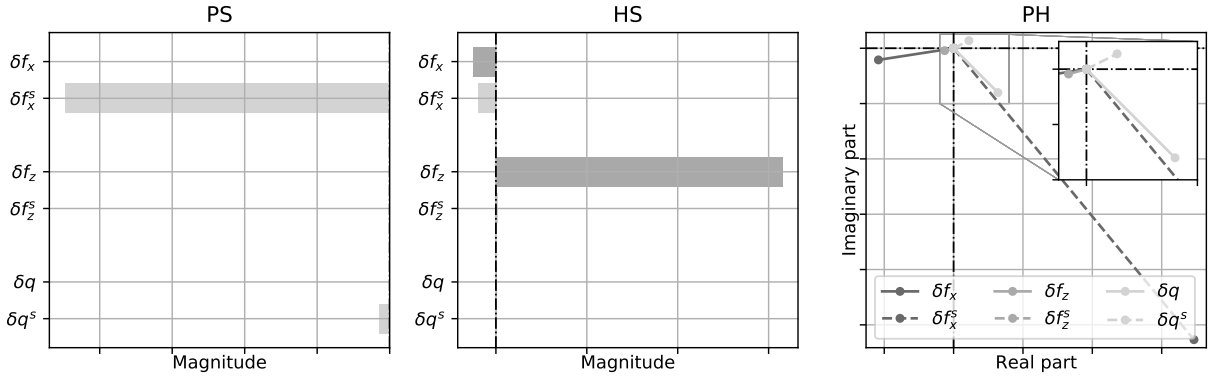


(c) PHM

Figure 6: Modal distortion induced by the MCA for different motion cueing configurations.

**Design for pitch subsidence (APM)** Figure 6a shows the modal distortion induced by a motion cueing configuration designed to minimize distortion of the aperiodic pitch mode, or pitch subsidence (PS). It can be seen that the this mode is reproduced almost one-to-one in the simulator, because the dark and light grey bars are aligned. This is achieved primarily by nulling the high-pass pitch filter and by finding an appropriate balance in the settings of the high-pass surge filter such to limit the resulting false cues in the $\delta f_x^s$. It can also be seen that the consequence of these settings is a significant distortion of both the phugoid and the heave subsidence modes. To prevent the violation of motion limits in heave, a moderate value for both the gain and break frequency of the high-pass heave filter were required. However, as can be seen from Figure 6a, this did not substantially affect the magnitude of $\delta f_z^s$ in the pitch subsidence mode.

Because of an implementation error, the first participating pilot flew a configuration with a value of $\omega_{n_x}$ of 1.3 rad/s instead of 1.25 rad/s. This results in the eigenvector corresponding to $\delta f_x^s$ to "flip" in sign w.r.t. $\delta f_x$ in Figure 6a, while the magnitude be-

comes slightly larger. During the experiment, the pilot comments in condition APM did not reflect this apparent sign change, yet the full impact on the experimental results remains unknown.

**Design for heave subsidence (AHM)** Figure 6b shows the modal distortion induced by the motion parameter set designed to mimimize distortion of the aperiodic heave mode, or heave subsidence (HS). It can be seen from the original mode shape (darker grey bars) that the vertical specific force is by far the most dominant. As such, it is possible to strongly limit motion in pitch and surge while still preserving this mode. This is also evident from the parameter set in Table 2, where both low gains and large values for the break-frequencies of the high-pass filters in surge and pitch are selected.

Due to the limited motion space of hexapod motion simulators in heave, it was also required to select a moderate value for the high-pass break-frequency in heave. This resulted in a strongly diminished amplitude of $\delta f_z^s$ with respect to $\delta f_z$, which was compensated by selecting a larger motion gain of 1.2. Using these settings, it can be seen from the figure that approximately half of the original contribution of $\delta f_z$ in the heave subsidence mode is preserved.

**Design for phugoid (PHM)** Figure 6c shows the modal distortion induced by the motion parameter set designed to mimimize distortion of the phugoid mode (PH). In hover, the phase difference between the longitudinal specific force and the pitch rate, the dominant contributors to this mode, is approximately ninety degrees. To preserve the phugoid mode shape, it is therefore desired to not only match the magnitudes of the perceived states as closely as possible, but also their *relative* phases. At the same time, the phase difference with respect to the original mode shape should be kept to a minimum, because this difference is effectively the mismatch between the *visual* and *motion* cues.

The motion parameter set shown in Figure 6c is a possible balance between these different requirements. It can be seen that the phase difference between $\delta f_x^s$ and $\delta q^s$ remains approximately ninety degrees. The phase differences with respect to the same quantities in the baseline vehicle model appears to be approximately ninety degrees as well. In terms of the magnitudes, it can be seen that $\delta q^s$ is substantially reduced with respect to the baseline value, while the magnitude of the $\delta f_z^s$ is increased. By far the most critical parameters that influence the magnitude of $\delta f_x^s$ in the phugoid mode were found to be the gain and high-pass break-frequency of the pitch filter. Enlarging the break-frequency of the pitch filter results in a smaller magnitude of the apparent *false cue* in $\delta f_x^s$, at the cost of a greater distortion in phase of both $\delta f_x^s$ and $\delta q^s$. Similarly, the pitch gain can be used to reduce the magnitude of the longitudinal specific force (more so than the gain on the longitudinal specific force). However, this also comes at the cost of a reduced magnitude of the simulated pitch rate. Note that, because of the seemingly strong false cue in $\delta f_x^s$, the pitch subsidence mode is also greatly distorted. Finally, because $\delta f_z$ does not significantly contribute to the phugoid mode, it has been opted to select the parameters in the heave channel such to strongly limit motion in heave and thereby use to freed motion space to cue the phugoid motion.

### 3.4. Hypotheses

Prior to the experiment, the following hypotheses, pertaining to dominant vehicle modes, task performance and pilot preference, were formulated:

1. It is hypothesized that the longitudinal and vertical position root mean squares (RMS's) in hover are smallest for the motion conditions APM and AHM, respectively, designed to best portray the hypothesized dominant vehicle modes. However, the position RMS's are foreseen to decrease in all conditions *with* motion when compared to the no-motion condition.

2. In the hover task performed, the dominant vehicle modes are hypothesized to be the pitch and heave subsidences. This is because a high-gain pilot strategy is anticipated, in which the phugoid has no time to develop. Hence, the overall MPFs corresponding to the pitch and heave subsidences are expected to be larger than the overall MPF corresponding to the phugoid mode.

3. Motion fidelity ratings are hypothesized to be more favourable for conditions APM and AHM (i.e., the expected dominant vehicle modes). Moreover, from prior experience it is expected that direct pitch motion feedback is valued most by pilots in the hover task and, therefore, motion fidelity ratings are expected to be most favourable for condition APM.

Hypothesis 1) stipulates that *all* conditions *with* motion cues are beneficial for the task when compared to the no-motion condition and that this will become evident from the position RMS's . Hypothesis 2) expresses that pilots are expected to benefit

most from motion cues that reproduce the faster vehicle modes, which are hypothesized to be dominant in the hover task. Finally, Hypothesis 3) expresses that pilots will also subjectively prefer the motion conditions corresponding to the dominant vehicle modes. Condition APM, which according to EMD reproduces the pitch subsidence mode one-to-one, is expected to be rated most favourably.

### 3.5. Dependent measures

Two primary dependent measures were collected during the experiment. First, time traces of vehicle model states were recorded. These are used to evaluate mode participation factors using Equation (6) and for longitudinal and vertical position error RMS's. Second, the Motion Fidelity Rating (MFR) scale[7] (see Figure 7) was used to quantify the subjective pilot preference for the various motion conditions evaluated. Repeated MFR scale ratings per motion condition are collected to allow for the evaluation of pilot consistency in the awarded ratings.

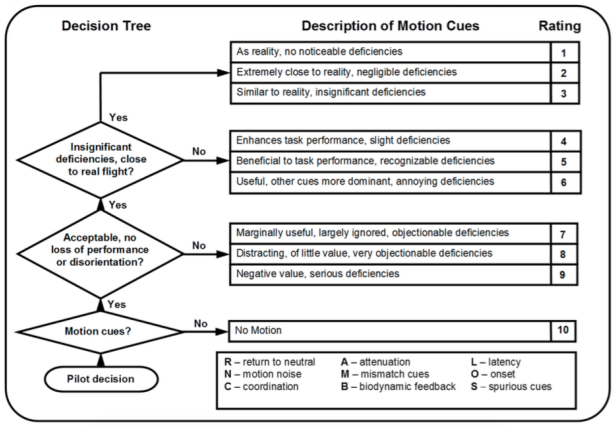


Figure 7: The Motion Fidelity Rating (MFR) scale[7].

### 3.6. Participants and procedure

The two participants that until the writing of this paper have performed the experiment are active military test pilots. The pilots were briefed regarding both the task to be performed and the MFR scale to be used for evaluating the various motion conditions. Each pilot underwent approximately twenty minutes of familiarization, where the task was repeated in each experiment condition until stable performance was attained. After familiarization, the actual experiment was initiated. Each condition (including the no motion condition) was assessed three times during the experiment. The respective repetitions were scheduled according to a Latin square design for each pilot as shown in Tables 3 and 4. Within each of the repetitions, three runs of the task were performed, after which a single MFR scale rating was given. In effect, each pilot experienced every motion condition for a total of *nine* times, yielding nine consecutive pilot input and vehicle state recordings as well as three MFR ratings per motion condition evaluated.

Table 3: Experiment conditions for pilot 1.

| Repetition | Conditions | | | |
|---|---|---|---|---|
| 1 | AHM | PHM | APM | NM |
| 2 | PHM | NM | AHM | APM |
| 3 | APM | AHM | NM | PHM |

Table 4: Experiment conditions for pilot 2.

| Repetition | Conditions | | | |
|---|---|---|---|---|
| 1 | AHM | NM | APM | PHM |
| 2 | NM | AHM | PHM | APM |
| 3 | APM | PHM | NM | AHM |

## 4 RESULTS

The following sections present the results obtained for each of the dependent measures collected during the experiment.

### 4.1. Position error

Figure 8 shows the root mean squared (RMS) in feet, denoted by $\sigma$, of the longitudinal and vertical position error per experimental condition. A separate figure is included for each of the two pilots.

In general, vertical position RMS's are significantly smaller in magnitude than longitudinal position RMS's. Also, the spread within and across conditions in the longitudinal position RMS's is larger than the spread in the vertical position RMS's. This result is true for both pilots, which suggests that maintaining altitude is easier than maintaining longitudinal position. This is explained in part by the vehicle dynamics (i.e. unstable phugoid), but also by the available visual cues. Namely, the hover board provides direct visual feedback regarding altitude, whereas longitudinal position is discernible only from inspection of the relative orientation of the pylons on the right (see Figure 4).

For both pilots, the position RMS's in conditions NM and PHM are comparable, with pilot 2 exhibiting a somewhat larger spread of the results, particularly in condition PHM. However, more substantial differences in the results between the two pilots are seen when comparing conditions APM and

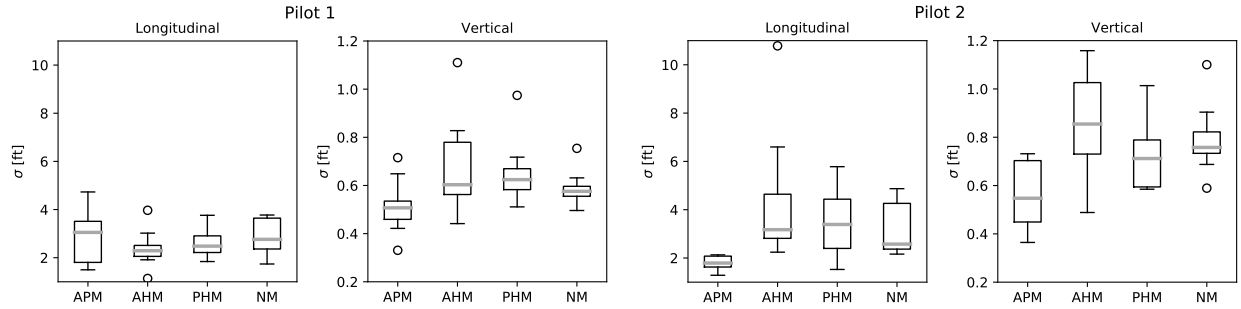


Figure 8: Horizontal and vertical position RMS's for pilot 1 (left) and pilot 2 (right) per experimental condition

AHM. For pilot 1, the difference between these conditions is marginal, and perhaps even in favor of condition AHM when considering longitudinal position. However, for pilot 2, both the median value and spread in the longitudinal position RMS's are substantially smaller in condition APM in comparison to condition AHM, but also in comparison to conditions PHM and NM.

Reflecting on the hypotheses, it appears that hypothesis 1) is rejected based on the results presented. Insignificant differences, in the order of tenths of feet, in median vertical position RMS's are observed for both pilots across all experimental conditions. The spread in the vertical position RMS's for both pilots, however, is larger in condition AHM as compared to the other conditions. Also, position error is not necessarily better in conditions with motion as compared to the no-motion condition. When considering longitudinal position RMS's, pilot 2 does seem to strongly benefit from pitch motion cues in condition APM, particularly for maintaining longitudinal position, but also vertical position. This, however, is not confirmed by the results of pilot 1, which show a slightly *larger* median and spread in the longitudinal position RMS's corresponding to condition APM.

### 4.2. Mode participation factors

Figure 9 shows the mode participation factors (MPFs) per experimental condition. As explained in Section 2, the MPF is a measure of the contribution of each vehicle mode in the overall vehicle response. A separate figure is included for each of the two pilots.

From the figure, it can be seen that the absolute values and spreads of the MPFs of each mode across experimental conditions vary. Interestingly however, when considering the *median* MPFs the relative contribution of each mode remains constant across conditions. The phugoid (PH) mode appears to dominate the vehicle response, followed by the pitch (PS) and heave subsidence (HS), respectively. Another result common to both pilots is that the *absolute* values of the MPFs corresponding to the phugoid (PH) and pitch subsidence (PS) are substantially larger in absolute value for condition AHM than for the other experimental conditions. This indicates that the excitation of these modes is stronger when pitch and surge motion cues are absent. From Figure 8, it is furthermore concluded that the stronger excitation of the phugoid and pitch subsidence modes in condition AHM does not necessarily result in a larger longitudinal position error.

Observing the results for each pilot individually, some interesting remarks can also be made. For pilot 1, it appears from the median MPFs that the presence of (one-to-one) pitch motion cues results in a larger participation of the phugoid (PH) and pitch subsidence (PS) modes. This is especially true in comparison to conditions PHM and NM, where the median MPFs of the phugoid (PH) and pitch subsidence (PS) are smaller. With the exception of condition AHM, the differences in the MPFs across conditions for pilot 1 seem minor.

For pilot 2, the opposite is true, where the median and spread in the MPFs indicate a smaller participation of the phugoid (PH) and pitch subsidence (PS) in condition APM when compared to conditions PHM and NM. This result is in strong agreement with Figure 8, where it was found that the RMS of the longitudinal position for pilot 2 in condition APM was substantially less than in the other conditions.

Reflecting on the hypotheses, it appears that hypothesis 2) must be rejected. Instead of the pitch and heave subsidences, the unstable phugoid mode contributes most to the vehicle response in all conditions evaluated. Furthermore, the results suggest that pilot control behaviour is strongly affected by both the presence and absence of pitch motion cues.

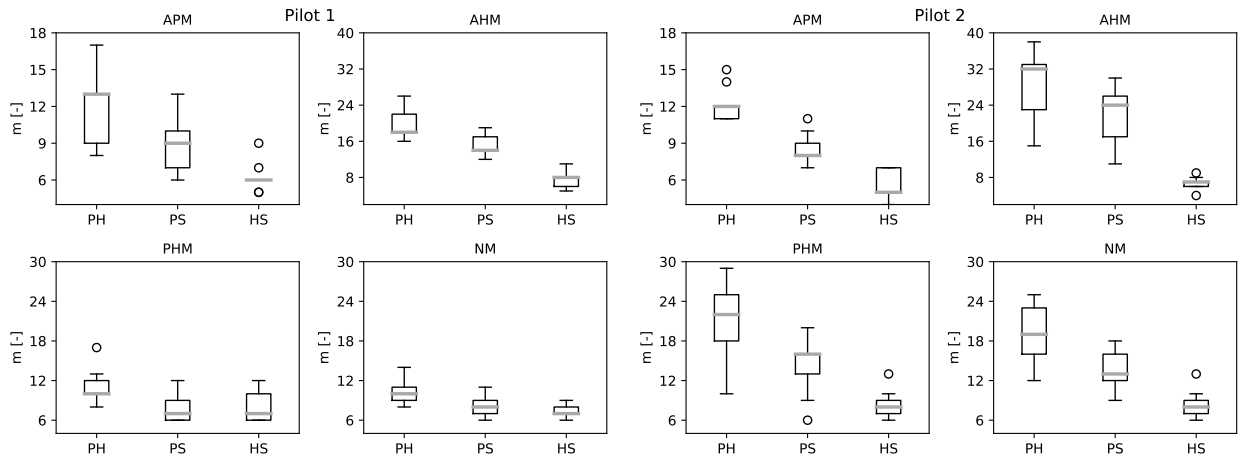


Figure 9: Mode participation factors for pilot 1 (left) and pilot 2 (right) per experimental condition.

### 4.3. Pilot ratings

Figure 10 shows the repeated MFR ratings awarded by each pilot per experimental condition. As discussed in Section 3, three separate ratings for each individual experimental condition and pilot are available. Figure 10 therefore also shows the medians and spread.

Pilot 1 seems to prefer condition PHM over conditions AHM and APM. However, in the third repetition of PHM, a significantly degraded rating was awarded. Condition APM, in contrast, is rated only slightly worse than PHM with a median of 5 and a worst rating of 6. Therefore, it seems inconclusive which of the two conditions (APM or PHM) is the overall preferred by pilot 1. It is also evident that condition AHM is not appreciated by pilot 1, citing heave cues as being too over-present and a strong lack of longitudinal (pitch) motion cues. Pilot 1 furthermore correctly identified the no-motion (NM) conditions in each repetition.

Pilot 2 clearly prefers condition APM over conditions PHM and AHM as evidenced by the median MFR rating of 2 and a worse rating of 3. Interestingly, pilot 2 also prefers the no-motion (NM) condition over PHM and AHM as evidenced by the corresponding median MFR ratings in the first two repetitions. Only in the third repetition of NM the pilot reported to not have perceived any motion. Next to the no-motion condition, the worst rated condition with motion seems AHM, where like pilot 1, pilot 2 also commented on the lack of pitch cues and over-dominant heave cues.

Reflecting on the hypotheses, the results from this experiment seem to partially confirm hypothesis 3) in that APM is the motion condition with the (overall) most favourable MFR ratings. The pitch subsidence mode best reproduced in condition APM, however, is not the dominant vehicle mode. Hence, the expectation that a motion cueing configuration based on preserving the dominant vehicle mode is *objectively* better seems discrepant. Also, the hypothesis that condition AHM would also receive favourable MFR ratings is false. Pilot ratings for condition AHM are (overall) worse than condition PHM and (in case of pilot 2) even the no-motion (NM) condition. This is also supported by pilot comments, which clearly indicate the lack of pitch motion cues in condition AHM as detrimental to perceived motion fidelity.

## 5 DISCUSSION

The present paper has investigated the utility of the novel *eigenmode distortion* (EMD) methodology for the configuration of motion cueing algorithms (MCAs) in helicopter flight simulation. Two experienced test pilots participated in a experiment where a precision hover task was performed in different motion cueing configurations, each devised to best reproduce one of the three (longitudinal) vehicle modes in accordance with the EMD methodology.

The results from this experiment show that task performance, in terms of longitudinal and vertical position root mean square (RMS), is not consistently affected by motion cues. One pilot showed a clear benefit of pitch motion cues in reducing longitudinal position error. The other pilot's task performance, however, was almost constant across all conditions evaluated and, if anything, seemed to degrade slightly with the presence of higher fidelity pitch motion cues.

In terms of the identified dominant vehicle modes, it was found that the unstable phugoid mode, in all experimental conditions evaluated, has the largest relative participation. This suggests that

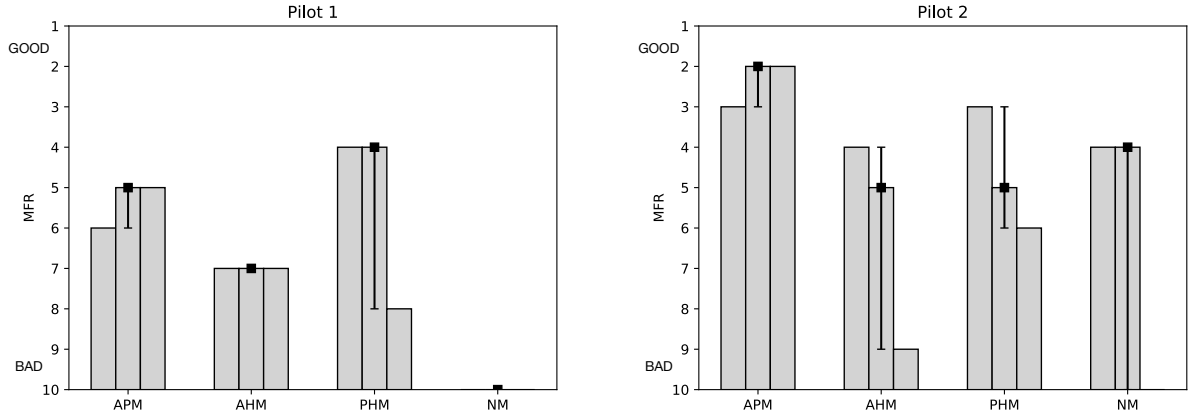


Figure 10: Repeated MFR ratings awarded by each pilot for each motion condition.

pilots may have adopted a relatively low-gain control strategy, where excitation of the unstable vehicle dynamics was avoided. The free (longer-term) response of the vehicle is then governed by the phugoid mode, which explains its relatively larger contribution to the overall dynamic response. Another interesting finding is that participation of the phugoid and pitch subsidence are larger in absolute value in the condition where predominantly vertical motion cues were offered (i.e., AHM). Also, one pilot seemed to benefit substantially more from pitch motion cues than the other. This suggests that the excitation of vehicle dynamics and, by extension, pilot control behaviour, changes with the presence or absence of motion cues in certain degrees-of-freedom, even though task performance is not necessarily affected.

The final metric collected during the experiment were the subjective pilot ratings based on the Motion Fidelity Rating (MFR) scale[7]. Of the three conditions with motion, it was found that the condition with only vertical motion cues (i.e., AHM) was rated least favourably, where both pilots noticed and commented on the lack of pitch motion cues. The condition designed to reproduce the pitch subsidence mode one-to-one (i.e., APM), was rated most favourably on the overall. However, the pitch subsidence is *not* the dominant vehicle mode. Hence, a motion cueing configuration based on the dominant vehicle mode (i.e., in this case, PHM) is not necessarily one that is also favoured most by pilots. In several trials, however, one pilot did express a preference for the phugoid optimized condition (i.e., PHM) over condition APM. These combined results suggest that, for the hover task evaluated, pilots value longitudinal (pitch) motion cues more than *only* heave motion cues.

Summarizing, the present experiment has resulted in a number of interesting findings that will serve as a basis for further research. The EMD methodology applied in the design of the evaluated motion cueing configurations has also shown promise as an objective guide in tuning motion cueing algorithms. However, more research is necessary to establish effective tuning strategies based on the EMD methodology. The experiment described in this paper will also be repeated with more pilots. Moreover, more dynamic tasks like the acceleration-deceleration or lateral reposition manoeuvres will be considered for more thorough comparison of different motion cueing strategies. Finally, the methodology will be extended to six (rigid-body) degrees-of-freedom.

## 6 CONCLUSION

The present paper applied a new approach, *eigenmode distortion* (EMD), to the motion cueing fidelity problem in helicopter flight simulation. The methodology, demonstrated for the first time in an experiment executed on the SIMONA Research Simulator at Delft University of Technology, has shown promise as an objective guide for tuning motion cueing algorithms. It is applicable to any task, vehicle and simulator combination.

Future work is necessary on the development of effective tuning strategies based on EMD. Also, the method will be extended to other and more helicopter degrees-of-freedom. Finally, more dynamic tasks will be considered using a similar approach as the one presented in this paper and with more participating pilots.

## REFERENCES


[1] S. K. Advani, R. J. A. W. Hosman, and M. Potter. Objective Motion Fidelity Qualification in Flight Training Simulators. In *AIAA Modeling and Simulation Technologies Conference and Exhibit*, number AIAA 2007-6802, 20 - 23 August 2007.

[2] Anonymous. Aeronautical Design Standard-33E-PRF, performance specification, handling qualities requirements for military rotorcraft. Technical report, US Army AMCOM, Redstone, Alabama, USA, March 2000.

[3] Anonymous. ICAO 9625: Manual of Criteria for the Qualification of Flight Simulation Training Devices. Volume 1: Aeroplanes. Technical report, International Civil Aviation Authority, 2009. Third Edition.

[4] C. Chalk, T.P. Neal, T.M. Harris, F. E. Pritchard, and R. J. Woodcock. Background Information and User Guide for MIL-F–8785B(ASG): Military Specification-Flying Qualities of Piloted Airplanes. Technical Report AFWAL-TR-81-3109, Flight Dynamics Laboratory, Air Force Wright Aeronautical Libraries, 1969.

[5] W. Dalmeijer, I. Miletović, O. Stroosma, and M. D. Pavel. Extending the Objective Motion Cueing Test to Measure Rotorcraft Simulator Motion Characteristics. In *Proceedings of the AHS 73rd Annual Forum, Fort Worth (TX), May 9-11*, pages 1876–1891, 2017.

[6] K. de Ridder and M. Roza. Automatic optimization of motion drive algorithms using objective motion cueing tests. In *AIAA Modeling and Simulation Technologies Conference, Kissimmee, FL*, 2015.

[7] S. J. Hodge, P. S. Perfect, G. D. Padfield, and M. D. White. Optimising the Vestibular Cues Available from a Short Stroke Hexapod Motion Platform. In *67th Annual Forum of the American Helicotper Society, Virginia Beach, VA, USA, May 3-5*, 2011.

[8] R. J. A. W. Hosman and S. K. Advani. Design and evaluation of the objective motion cueing test and criterion. *The Aeronautical Journal*, 120(1227):873–891, 2016.

[9] R. J. A. W. Hosman, S. K. Advani, and J. Takats. Status of the ICAO Objective Motion Cueing Test. In *Autumn Flight Simulation Conference: Flight Simulation Research - New Frontiers*. Royal Aeronautical Society, Royal Aeronautical Society, November 2012.

[10] M. Jones. Optimizing the Fitness of Motion Cueing for Rotorcraft Flight Simulation. In *Proceedings of the AHS 72nd Annual Forum, West Palm Beach (FL), May 17-19*. American Helicopter Society International, Inc., 2016.

[11] M. Jones, M. D. White, T. Fell, and M. Barnett. Analysis of motion parameter variations for rotorcraft flight simulators. In *Proceedings of the AHS 73rd Annual Forum, Fort Worth (TX), May 9-11*, 2017.

[12] I. Miletović, M. D. Pavel, O. Stroosma, D. M. Pool, M. M. Van Paassen, M. Wentink, and M. Mulder. Motion cueing fidelity in flight simulation: A novel perspective. *To be submitted*, 2018.

[13] A. V. Oppenheim and G. C. Verghese. *Signals, System & Inference*. Pearson, 2015.

[14] G. D. Padfield. *Helicopter Flight Dynamics: The Theory and Application of Flying Qualities and Simulation Modelling*. Blackwell Publishing, 2 edition, 2007.

[15] D. M. Pool. *Objective Evaluation of Flight Simulator Motion Cueing Fidelity Through a Cybernetic Approach*. PhD thesis, Delft University of Technology, Faculty of Aerospace Engineering, September 2012.

[16] S. E. Reardon and S. D. Beard. Evaluation of Motion Tuning Methods on the Vertical Motion Simulator. In *Proceedings of the AHS 71st Annual Forum, Virginia Beach (VA)*, May 2015.

[17] L. D. Reid and M. A. Nahon. Flight Simulation Motion-Base Drive Algorithms. Part 1: Developing and Testing the Equations. Technical Report UTIAS 296, University of Toronto, Institute for Aerospace Studies, December 1985.

[18] J. A. Schroeder. Helicopter Flight Simulation Motion Platform Requirements. Technical Report TP-1999-208766, NASA, Moffett Field, California, July 1999.

[19] J. B. Sinacori. The Determination of Some Requirements for a Helicopter Research Simulation Facility. Technical Report NASA-CR-152066, Systems Technology Inc., September 1977.

[20] F. A. M. van der Steen. *Self-Motion Perception*. PhD thesis, Delft University of Technology, Faculty of Aerospace Engineering, 1998.

[21] P. M. T. Zaal, J. A. Schroeder, and W. W. Y. Chung. Objective Motion Cueing Criteria Investigation Based on Three Flight Tasks. In *Proceedings of the RAeS Flight Simulation Conference, 9-10 June 2015, London, UK*. Royal Aeronautical Society, June 2015.